An Energy-Based Framework for Nonlinear Kinetostatic Modeling of Compliant Mechanisms Utilizing Beam Flexures

Guimin Chen*
Professor
State Key Laboratory for
Systems Engineering
Shaanxi Key Lab of
Intelligent Robots
Xi'an Jiaotong University
Xi'an, Shaanxi 710049, China
Email: guimin.chen@gmail.com

Fulei Ma
Lecturer
School of Electro-Mechanical
Engineering, Xidian University
Xi'an, Shaanxi 710071, China
Email: fuleima@gmail.com

Ruiyu Bai
Ph.D Candidate
School of Electro-Mechanical
Engineering, Xidian University
Xi'an, Shaanxi 710071, China
Email: 1506559641@qq.com

Weidong Zhu
Professor, Fellow of ASME
Department of Mechanical Engineering
University of Maryland
Baltimore County, Baltimore, MD 21250, USA
Email: wzhu@umbc.edu

Spencer P. Magleby
Professor
Mechanical Engineering Department
Brigham Young University
Provo, UT 84602, USA
Email: magleby@byu.edu

Larry L. Howell
Professor, Fellow of ASME
Mechanical Engineering Department
Brigham Young University
Provo, UT 84602, USA
Email: lhowell@byu.edu

*Address all correspondence to this author.

ABSTRACT

Although energy-based methods have advantages over the Newtonian methods for kinetostatic modeling, the geometric nonlinearities inherent in deflections of compliant mechanisms preclude most of the energy-based theorems. Castigliano's first theorem and the Crotti-Engesser theorem, which don't require the problem being solved to be linear, are selected to construct the energy-based kinetostatic modeling framework for compliant mechanisms in this work. Utilization of these two theorems requires explicitly formulating the strain energy in terms of deflections and the complementary strain energy in terms of loads, which are derived based on the beam constraint model. The kinetostatic modeling of two compliant mechanisms are provided to demonstrate the effectiveness of the explicit formulations in this framework derived from Castigliano's first theorem and the Crotti-Engesser theorem.

1 Introduction

Compliant mechanisms, which achieve at least some of their mobility from the deflection of flexible segments rather than from articulated joints only, offer many advantages such as energy storage, increased precision, and reduced wear, backlash and part number [1]. Because the motion of a compliant mechanism involves elastic deflections, kinematic analysis should be accompanied by static analysis to determine the relation between loads and resulting mechanism motion [2]. The combination of kinematic analysis and static analysis is termed kinetostatic modeling.

Similar to static structural mechanics, various kinetostatic modeling methods of compliant mechanisms can be roughly grouped into two categories. The first group, known as Newtonian methods (or vectorial methods), require all the internal forces and displacements to be considered [3, 4], thus making the modeling process time-consuming and error-prone. Although nonlinear finite element models (NFEMs) are useful for analyzing nonlinear deflections of compliant mechanisms, but they provide little parametric design insight. NFEMs could yield wrong mode bending for flexible beams experiencing compressive-force dominant loads, especially when the tip deflections are given [3,5]. The second group is the strain-energy methods. Because strain energy is a scalar quantity (thus is independent of the coordinate frame), it provides a convenient way for capturing the kinetostatic behaviors of compliant mechanisms [6–8]. When using energy-based methods, a compliant mechanism is viewed in its entirety and one can neglect the load equilibriums of the internal loads between its adjacent elements [9]. Although strain-energy methods are favorable in many situations, the inherent geometric nonlinearities of compliant mechanisms preclude the use of most of the available energy theorems. For example, the dummy load method [10, 11] was employed to identify deflection and sensitivity information of compliant mechanisms, the mutual potential energy [12] was employed to formulate the objective for topology optimization of ground structure-based compliant mechanisms, and Castigliano's second theorem [13] was utilized to derive the compliance factors of various flexure hinges, both of which assumed the problems were linear elastic. Eastwood et al. [14] employed Castigliano's first theorem to solve the static behavior of nitinol notched-tube joints considering material nonlinearity without geometrical nonlinearity.

The objective of this work is to construct an energy-based framework for modeling nonlinear kinetostatics of compliant mechanisms. Such a framework should be able to determine the displacements of nonlinear deflections for given loads from energies, and vice versa. Fortunately, there are two dual theorems that don't require the problem to be linear, i.e., Castigliano's first theorem and the Crotti-Engesser theorem [15–17]. Castigliano's first theorem can be used to determine loads

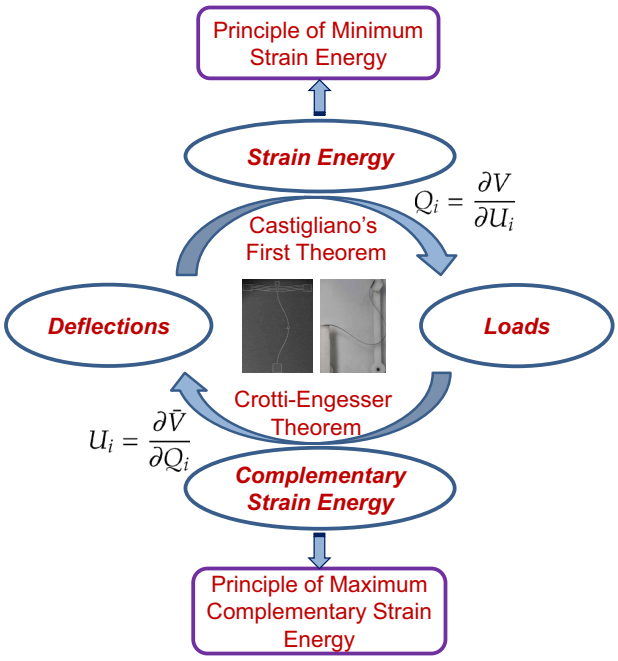

Fig. 1. The energy-based kinetostatic modeling framework for compliant mechanisms.

from strain energy for given displacements, while the Crotti-Engesser theorem achieves displacements from complementary strain energy for given loads, as will be briefly introduced in Section 2. The two theorems are chosen for constructing the energy-based kinetostatic modeling framework for compliant mechanisms, as illustrated in Figure 1. Among the framework in Figure 1, the principle of minimum strain energy and the principle of minimum complementary strain energy will be left for future discussion. Figure 2 plots a nonlinear load-deflection curve for a cantilever beam subject to tip loads. The load-deflection curve divides the box into two regions, the region beneath the curve and the region above the curve. The area of the region under the curve is the strain energy, while the area of the region above the curve is the complementary strain energy [16]. Although the complementary strain has no physical meaning, it is critical in forming the proposed energy-based framework.

Another challenge for the energy-based framework lies in explicitly formulating the energies in compliant mechanisms. Utilization of the theorems requires explicitly expressing the strain energy in terms of deflections while the complementary strain energy in terms of loads, which will be another contribution of this work. The pseudo-rigid-body model (PRBM) [1] offers an easy way to calculate the strain energy stored in a compliant mechanism (by adding up the energies stored in the equivalent springs at all the pseudo joints). For example, Jensen et al. [18, 19] used PRBM-based strain energy expression to identify multistable configurations and to solve for the kinetostatic behaviors, and Turkkan and Su [2] developed a conceptual design tool for compliant mechanisms called DAS-2D in which PRBM-based strain energy formulation combined with a minimization energy scheme was employed, which was further adopted by Venkiteswaran et al. [20] for topology optimization of compliant mechanisms. However, inherent lumped-compliance assumptions lead to relative large errors for energy calculations [21, 22]. Interestingly, based on the beam constraint model (BCM) [23], Awtar and Sen [9] derived an explicit strain energy expression, which inspires us to construct the energy-based framework based on BCM. BCM has been

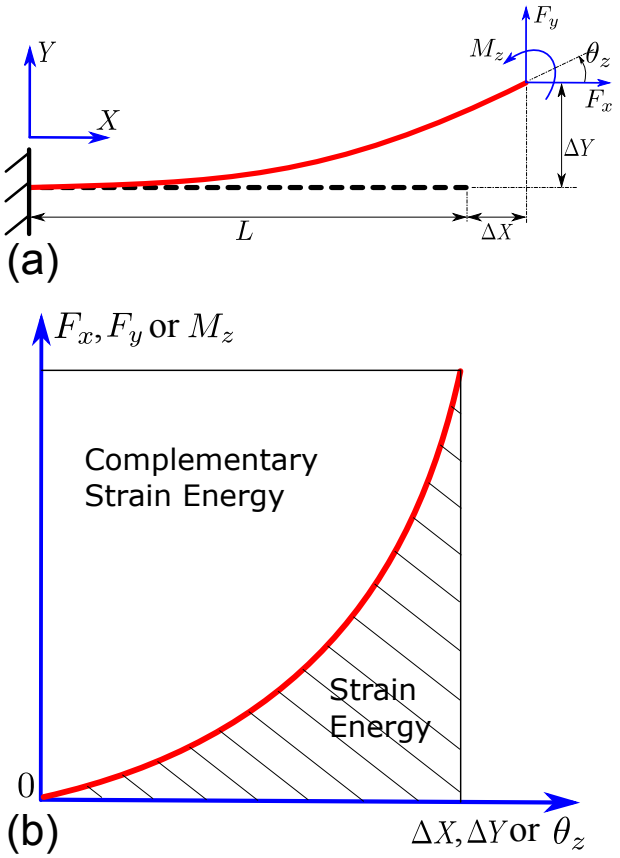

Fig. 2. A cantilever beam subject to combined force and moment loads and illustration of the corresponding strain energy and complementary strain energy.

extended for different modeling scenarios of nonlinear deflections [3, 24–26], which makes the framework extensible.

To sum up, we propose an energy-based framework that integrates both strain energy and complementary strain energy for nonlinear kinetostatic modeling of compliant mechanisms. Within the framework, the strain energy and complementary strain energy are expressed in closed-form using the BCM and integrated by two nonlinear energy theorems, i.e., Castigliano's first theorem and the Crotti-Engesser theorem. Such a framework provides new insights for designers to model and understand nonlinear kinetostatic behaviors of compliant mechanisms. The framework is extendable for modeling large deflections by following the idea of CBCM [3, 24] and incorporating the principle of minimum energy and the principle of minimum complementary energy, thus setting a foundation for future work.

The outline of this work is as follows. Section 2 briefly reviews the two energy theorems. Section 3 derives the strain energy and complementary strain energy expressed in a form that can be directly integrated with the two energy theorems based on the beam constraint model (BCM) [23]. Section 4 incorporates two compliant mechanism examples to demonstrate the use of the two energy theorems on the derived expressions for strain energy and complementary strain energy.

Table 1. Beam characteristic coefficients of BCM matrices [23]

$k_{11}^{(0)}$	$k_{12}^{(0)}$	$k_{22}^{(0)}$	$k_{11}^{(1)}$	$k_{12}^{(1)}$	$k_{22}^{(1)}$	$k_{11}^{(2)}$	$k_{12}^{(2)}$	$k_{22}^{(2)}$
12	-6	4	6/5	-1/10	2/15	-1/700	1/1400	-11/6300

2 Two Energy Theorems for Nonlinear Elastic Systems

Although this work only discusses geometrically nonlinear problems in which linear elastic materials are assumed, the use of the following two energy theorems can be extended for problems of material nonlinearities (e.g., stress-strain relation given as $\sigma = \sqrt{\varepsilon}$).

2.1 Castigliano's First Theorem (Strain Energy)

Suppose the strain energy stored in an elastic structure is V. Castigliano's first theorem (derived from the Principle of Virtual Work) states that, if the strain energy of an elastic structure can be expressed as a function of generalized displacement U_i (for planar deflections, U_i may be Δ_x, Δ_y or δ_θ), then the partial derivative of the strain energy with respect to the generalized displacement gives the generalized force Q_i (F_x, F_y or M_z), that is,

$$Q_i = \frac{\partial V}{\partial U_i} \tag{1}$$

where U_i is the deflection at the point of application of force Q_i in the direction of Q_i (if U_i is a rotation, Q_i will be a moment at the point).

2.2 Crotti-Engesser Theorem (Complementary Strain Energy)

The Crotti-Engesser theorem, also called the generalized Castigliano's second theorem, was derived from the Principle of Complementary Virtual Work. It states that if the strain energy of an elastic structure can be expressed as a function of generalized force Q_i, then the partial derivative of the complementary strain energy with respect to the generalized force gives the generalized displacement U_i, that is,

$$U_i = \frac{\partial \bar{V}}{\partial Q_i} \tag{2}$$

where U_i is the deflection at the point of application of force Q_i in the direction of Q_i, and $\bar{V}$ is the complementary strain energy (as illustrated in Figure 2).

For the special case of linear elasticity, the strain energy and the complementary energy of the system are equal and interchangeable.

3 Formulating Strain Energy and Complementary Strain Energy in Deflected Beams

To take advantage of these two energy theorems, we need to explicitly express the strain energy and the complementary strain energy in a deflected beam. The beam constraint model (BCM) [23] is chosen to obtain the closed-form expressions

because of its capability of capturing relevant geometric nonlinearities.

The basic formulations of the BCM from Ref. [23] are briefly summarized below. Figure 2 shows a simple cantilever beam of uniform cross-section whose length is L, in-plane thickness is T, and out-of-plane thickness is W. $A = WT$ and $I = WT^3/12$ denote the area (A) and the second moment of inertia (I) of the beam's cross-section, respectively. The Young's modulus of the material for the beam is denoted as E. The beam is subject to a transverse force F_y, an axial force F_x and a moment M_z at its free end, resulting in axial and transverse deflections ΔX and ΔY and tip slope θ_z. For the transverse deflection and the tip slope within $0.1L$ and 0.1 Rad, respectively, the BCM carries out a partial linearization of the Euler-Bernoulli beam equation (i.e., linearizing the expression for curvature while formulating the load equilibrium expression in the deformed beam configuration) then expands (using the Taylor series) and truncates the result to yield the simplified load-deflection relations for the beam [23]:

$$\begin{bmatrix} f_y \\ m_z \end{bmatrix} = \begin{bmatrix} k_{11}^{(0)} & k_{12}^{(0)} \\ k_{12}^{(0)} & k_{22}^{(0)} \end{bmatrix} \begin{bmatrix} u_y \\ \theta_z \end{bmatrix} + f_x \begin{bmatrix} k_{11}^{(1)} & k_{12}^{(1)} \\ k_{12}^{(1)} & k_{22}^{(1)} \end{bmatrix} \begin{bmatrix} u_y \\ \theta_z \end{bmatrix} + f_x^2 \begin{bmatrix} k_{11}^{(2)} & k_{12}^{(2)} \\ k_{12}^{(2)} & k_{22}^{(2)} \end{bmatrix} \begin{bmatrix} u_y \\ \theta_z \end{bmatrix} \tag{3}$$

and

$$u_x = \frac{f_x}{k_a} - \frac{1}{2} \begin{bmatrix} u_y & \theta_z \end{bmatrix} \begin{bmatrix} k_{11}^{(1)} & k_{12}^{(1)} \\ k_{12}^{(1)} & k_{22}^{(1)} \end{bmatrix} \begin{bmatrix} u_y \\ \theta_z \end{bmatrix} - f_x \begin{bmatrix} u_y & \theta_z \end{bmatrix} \begin{bmatrix} k_{11}^{(2)} & k_{12}^{(2)} \\ k_{12}^{(2)} & k_{22}^{(2)} \end{bmatrix} \begin{bmatrix} u_y \\ \theta_z \end{bmatrix} \tag{4}$$

where $k_a = 12L^2/T^2$, the normalized load and deflection parameters (represented by lower case letters) are defined as

$$m_z = \frac{M_z L}{EI},\ f_y = \frac{F_y L^2}{EI},\ f_x = \frac{F_x L^2}{EI},\ u_y = \frac{\Delta Y}{L},\ u_x = \frac{\Delta X}{L} \tag{5}$$

and the k's in the matrices are referred to as the beam characteristic coefficients, whose values are listed in Table 1.

3.1 Strain Energy

The strain energy can be expressed by BCM as [9]

$$v = \frac{f_x^2}{2k_a} + \frac{1}{2} \begin{bmatrix} u_y & \theta_z \end{bmatrix} \begin{bmatrix} k_{11}^{(0)} & k_{12}^{(0)} \\ k_{12}^{(0)} & k_{22}^{(0)} \end{bmatrix} \begin{bmatrix} u_y \\ \theta_z \end{bmatrix} - \frac{f_x^2}{2} \begin{bmatrix} u_y & \theta_z \end{bmatrix} \begin{bmatrix} k_{11}^{(2)} & k_{12}^{(2)} \\ k_{12}^{(2)} & k_{22}^{(2)} \end{bmatrix} \begin{bmatrix} u_y \\ \theta_z \end{bmatrix} \tag{6}$$

where v denotes the normalized strain energy, and the actual strain energy stored in the beam can be calculated using $V = vEI/L$. By defining

$$S^{(j)} = \begin{bmatrix} u_y & \theta_z \end{bmatrix} \begin{bmatrix} k_{11}^{(j)} & k_{12}^{(j)} \\ k_{12}^{(j)} & k_{22}^{(j)} \end{bmatrix} \begin{bmatrix} u_y \\ \theta_z \end{bmatrix} = k_{11}^{(j)} u_y^2 + 2k_{12}^{(j)} u_y \theta_z + k_{22}^{(j)} \theta_z^2 \qquad j = 0,1,2 \tag{7}$$

Eq. (6) can be simply denoted as

$$v = \frac{f_x^2}{2k_a} + \frac{S^{(0)}}{2} - \frac{f_x^2 S^{(2)}}{2} = \frac{f_x^2}{2} \left(\frac{1}{k_a} - S^{(2)} \right) + \frac{S^{(0)}}{2} \tag{8}$$

To take advantage of Castigliano's first theorem, the formulation should be rewritten in terms of the displacements. Eq. (4) can be rewritten as

$$u_x = \frac{f_x}{k_a} - \frac{S^{(1)}}{2} - f_x S^{(2)} \tag{9}$$

and we have

$$f_x \left(\frac{1}{k_a} - S^{(2)} \right) = u_x + \frac{S^{(1)}}{2} \tag{10}$$

Substituting Eq. (10) into Eq. (8) yields the following strain energy expression which is expressed in terms of the deflection parameters:

$$v = \frac{k_a (2u_x + S^{(1)})^2}{8(1 - k_a S^{(2)})} + \frac{S^{(0)}}{2} \tag{11}$$

This expression is consistent with the nonlinear strain energy expression of Eq. (43) in Ref. [9], except it is useful for deriving the expression for the complementary strain energy, as will be illustrated in the following.

3.2 Complementary Strain Energy

In this section we expand the BCM to include the complementary strain energy.

We define the sum of the strain energy and the complementary strain energy as the full strain energy, v^*. It can be seen from Figure 2 that the full strain energy depends only on the initial and the final states of the deflection process, irrespective of the order in which the loading is carried out. Because a given set of tip loads yields a unique set of tip deflections, the full strain energy can be calculated as

$$v^* = f_x u_x + \begin{bmatrix} f_y & m_z \end{bmatrix} \begin{bmatrix} u_y \\ \theta_z \end{bmatrix} \tag{12}$$

Substituting BCM's load-deflection relations, i.e., Eqs. (3) and (4) into Eq. (12) yields

$$\begin{aligned} v^* = & \frac{f_x^2}{k_a} - \frac{f_x}{2}\begin{bmatrix} u_y & \theta_z \end{bmatrix}\begin{bmatrix} k_{11}^{(1)} & k_{12}^{(1)} \\ k_{12}^{(1)} & k_{22}^{(1)} \end{bmatrix}\begin{bmatrix} u_y \\ \theta_z \end{bmatrix} - \\ & f_x^2\begin{bmatrix} u_y & \theta_z \end{bmatrix}\begin{bmatrix} k_{11}^{(2)} & k_{12}^{(2)} \\ k_{12}^{(2)} & k_{22}^{(2)} \end{bmatrix}\begin{bmatrix} u_y \\ \theta_z \end{bmatrix} + \begin{bmatrix} u_y & \theta_z \end{bmatrix}\begin{bmatrix} k_{11}^{(0)} & k_{12}^{(0)} \\ k_{12}^{(0)} & k_{22}^{(0)} \end{bmatrix}\begin{bmatrix} u_y \\ \theta_z \end{bmatrix} + \\ & f_x\begin{bmatrix} u_y & \theta_z \end{bmatrix}\begin{bmatrix} k_{11}^{(1)} & k_{12}^{(1)} \\ k_{12}^{(1)} & k_{22}^{(1)} \end{bmatrix}\begin{bmatrix} u_y \\ \theta_z \end{bmatrix} + f_x^2\begin{bmatrix} u_y & \theta_z \end{bmatrix}\begin{bmatrix} k_{11}^{(2)} & k_{12}^{(2)} \\ k_{12}^{(2)} & k_{22}^{(2)} \end{bmatrix}\begin{bmatrix} u_y \\ \theta_z \end{bmatrix} \\ = & \frac{f_x^2}{k_a} + \begin{bmatrix} u_y & \theta_z \end{bmatrix}\begin{bmatrix} k_{11}^{(0)} & k_{12}^{(0)} \\ k_{12}^{(0)} & k_{22}^{(0)} \end{bmatrix}\begin{bmatrix} u_y \\ \theta_z \end{bmatrix} + \frac{f_x}{2}\begin{bmatrix} u_y & \theta_z \end{bmatrix}\begin{bmatrix} k_{11}^{(1)} & k_{12}^{(1)} \\ k_{12}^{(1)} & k_{22}^{(1)} \end{bmatrix}\begin{bmatrix} u_y \\ \theta_z \end{bmatrix} \\ = & \frac{f_x^2}{k_a} + S^{(0)} + \frac{f_x S^{(1)}}{2} \end{aligned} \tag{13}$$

Then the complementary strain energy can be obtained by subtracting the strain energy given in Eq. (6) from the full strain energy in Eq. (13):

$$\begin{aligned} \bar{v} = v^* - v = & \frac{f_x^2}{2k_a} + \frac{1}{2}\begin{bmatrix} u_y & \theta_z \end{bmatrix}\begin{bmatrix} k_{11}^{(0)} & k_{12}^{(0)} \\ k_{12}^{(0)} & k_{22}^{(0)} \end{bmatrix}\begin{bmatrix} u_y \\ \theta_z \end{bmatrix} + \\ & \frac{f_x}{2}\begin{bmatrix} u_y & \theta_z \end{bmatrix}\begin{bmatrix} k_{11}^{(1)} & k_{12}^{(1)} \\ k_{12}^{(1)} & k_{22}^{(1)} \end{bmatrix}\begin{bmatrix} u_y \\ \theta_z \end{bmatrix} + \frac{f_x^2}{2}\begin{bmatrix} u_y & \theta_z \end{bmatrix}\begin{bmatrix} k_{11}^{(2)} & k_{12}^{(2)} \\ k_{12}^{(2)} & k_{22}^{(2)} \end{bmatrix}\begin{bmatrix} u_y \\ \theta_z \end{bmatrix} \\ = & \frac{f_x^2}{2k_a} + \frac{S^{(0)}}{2} + \frac{f_x S^{(1)}}{2} + \frac{f_x^2 S^{(2)}}{2} \end{aligned} \tag{14}$$

It should be noted that the first two terms of $\bar{v}$ and v are identical. These two terms correspond to the energy due to pure tension and pure bending, respectively, and no nonlinear couplings are included. The third and fourth terms of $\bar{v}$ capture the load-stiffening and elastokinematic effects, respectively.

To take advantage of the Crotti-Engesser theorem, the formulation of the complementary strain energy is required to be expressed in terms of the loads. Substituting the load-deflection relations in compliance matrix form from Ref. [23]

$$\begin{bmatrix} u_y \\ \theta_z \end{bmatrix} = \begin{bmatrix} \dfrac{r-\tanh k}{r^3} & \dfrac{\cosh r - 1}{r^2 \cosh r} \\ \dfrac{\cosh r - 1}{r^2 \cosh r} & \dfrac{\tanh r}{r} \end{bmatrix}\begin{bmatrix} f_y \\ m_z \end{bmatrix} \quad (r = \sqrt{f_x}) \tag{15}$$

into Eq. (14), and making a Taylor series expansion by retaining the terms up to the second power in f_x, we get

$$\begin{aligned} \bar{v} = & \frac{f_x^2}{2k_a} + \frac{1}{2}\begin{bmatrix} f_y & m_z \end{bmatrix}\begin{bmatrix} 1/3 & 1/2 \\ 1/2 & 1 \end{bmatrix}\begin{bmatrix} f_y \\ m_z \end{bmatrix} - \\ & \frac{1}{2} f_x \begin{bmatrix} f_y & m_z \end{bmatrix}\begin{bmatrix} 2/15 & 5/24 \\ 5/24 & 1/3 \end{bmatrix}\begin{bmatrix} f_y \\ m_z \end{bmatrix} + \\ & \frac{1}{2} f_x^2 \begin{bmatrix} f_y & m_z \end{bmatrix}\begin{bmatrix} 17/315 & 61/720 \\ 61/720 & 2/15 \end{bmatrix}\begin{bmatrix} f_y \\ m_z \end{bmatrix} \end{aligned} \tag{16}$$

or

$$\bar{v} = \frac{f_x^2}{2k_a} + \frac{1}{2}\begin{bmatrix} f_y & m_z \end{bmatrix}\begin{bmatrix} 1/3 & 1/2 \\ 1/2 & 1 \end{bmatrix}\begin{bmatrix} f_y \\ m_z \end{bmatrix} - \frac{1}{2}f_x\begin{bmatrix} f_y & m_z \end{bmatrix}\begin{bmatrix} 2/15 & 5/24 \\ 5/24 & 1/3 \end{bmatrix}\begin{bmatrix} f_y \\ m_z \end{bmatrix} + \frac{1}{2}f_x^2\begin{bmatrix} f_y & m_z \end{bmatrix}\begin{bmatrix} 17/315 & 61/720 \\ 61/720 & 2/15 \end{bmatrix}\begin{bmatrix} f_y \\ m_z \end{bmatrix} - \frac{1}{2}f_x^3\begin{bmatrix} f_y & m_z \end{bmatrix}\begin{bmatrix} 62/2835 & 277/8064 \\ 277/8064 & 17/315 \end{bmatrix}\begin{bmatrix} f_y \\ m_z \end{bmatrix} \tag{17}$$

if the terms up to the third power in f_x is retained. Eqs. (16) and (17) contains only the 3 load parameters, thus it can facilitate the use of the Crotti-Engesser theorem.

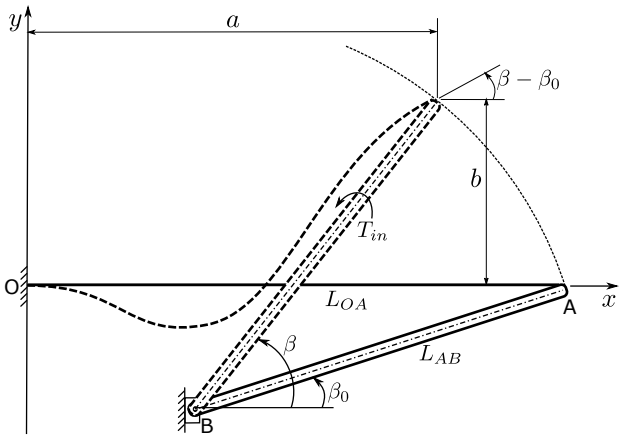

Fig. 3. Circular-guided compliant mechanism (beam OA is compliant and rigidly attached to the rigid crank AB).

4 Case Studies

This combination of Castigliano's first theorem, the Crotti-Engesser theorem, the beam constraint model, strain energy and complementary strain energy creates a framework for energy-based kinetostatic modeling of compliant mechanisms. Two case studies are presented to demonstrate the use of this framework.

4.1 Circular-Guided Compliant Mechanism

The circular-guided compliant mechanism (as shown in Figure 3) studied in Ref. [21] is chosen to demonstrate the use of Castigliano's first theorem. We take a special case of this mechanism in which the rigid crank is collinear with a compliant beam (OA in the undeflected position, or $\beta_0 = 0$), as shown in Figure 4. The angle between the crank and the x-axis is β. The

lengths of compliant beam OA and rigid crank AB are L_{OA} and L_{AB}, respectively. The in-plane thickness and the out-of-plane thickness of the compliant beam are T and W.

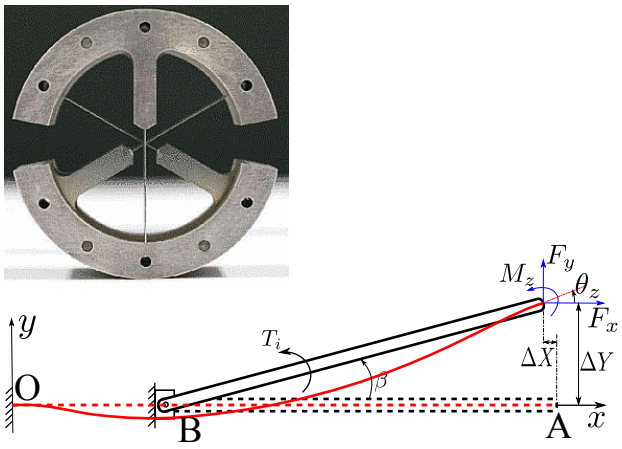

Fig. 4. The triple cross-spring flexure joint [27] and its simplified model derived from circular-guided compliant mechanisms.

The tip deflections are given as

$$\left.\begin{aligned} \Delta X &= u_x L_{OA} = L_{AB}(\cos\beta - 1) \\ \Delta Y &= u_y L_{OA} = L_{AB}\sin\beta \\ \theta_z &= \beta \end{aligned}\right\} \tag{18}$$

Differentiating with respect to β yields

$$\left.\begin{aligned} du_x &= -\frac{L_{AB}}{L_{OA}}\sin\beta d\beta \\ du_y &= \frac{L_{AB}}{L_{OA}}\cos\beta d\beta \\ d\theta_z &= d\beta \end{aligned}\right\} \tag{19}$$

Substituting Eq. (18) into Eq. (11) and differentiating with respect to β (Castigliano's first theorem) yields the required input torque to actuate the mechanism:

$$\begin{aligned} T_i = \frac{dv}{d\beta} &= k_{22}^{(0)}\beta + k_{12}^{(0)}R\sin\beta + R\cos\beta(k_{12}^{(0)}\beta + k_{11}^{(0)}R\sin\beta) - \\ &\frac{k_a Q_1[k_{22}^{(1)}\beta + (k_{12}^{(1)} - 1)R\sin\beta + R\cos\beta(k_{12}^{(1)}\beta + k_{11}^{(1)}R\sin\beta)]}{2Q_2} + \\ &\frac{k_a^2 Q_1^2[k_{22}^{(2)}\beta + k_{12}^{(2)}R\sin\beta + R\cos\beta(k_{12}^{(2)}\beta + k_{11}^{(2)}R\sin\beta)]}{4Q_2^2} \end{aligned} \tag{20}$$

Table 2. Parameters of the circular-guided compliant mechanism

E (Al7075-T6 alloy)	L_{OA}	L_{AB}	W	T	β_0
73 GPa	25 mm	21.8 mm	5.1 mm	0.25 mm	0

where

$$\left.\begin{aligned} R &= L_{AB}/L_{OA} \\ Q_1 &= -2R + k_{22}^{(1)}\beta^2 + 2R\cos\beta + 2k_{12}^{(1)}R\beta\sin\beta + k_{11}^{(1)}R^2\sin^2\beta \\ Q_2 &= -1 + k_{22}^{(2)}k_a\beta^2 + 2k_{12}^{(2)}k_aR\beta\sin\beta + k_{11}^{(2)}k_aR^2\sin^2\beta \end{aligned}\right\} \tag{21}$$

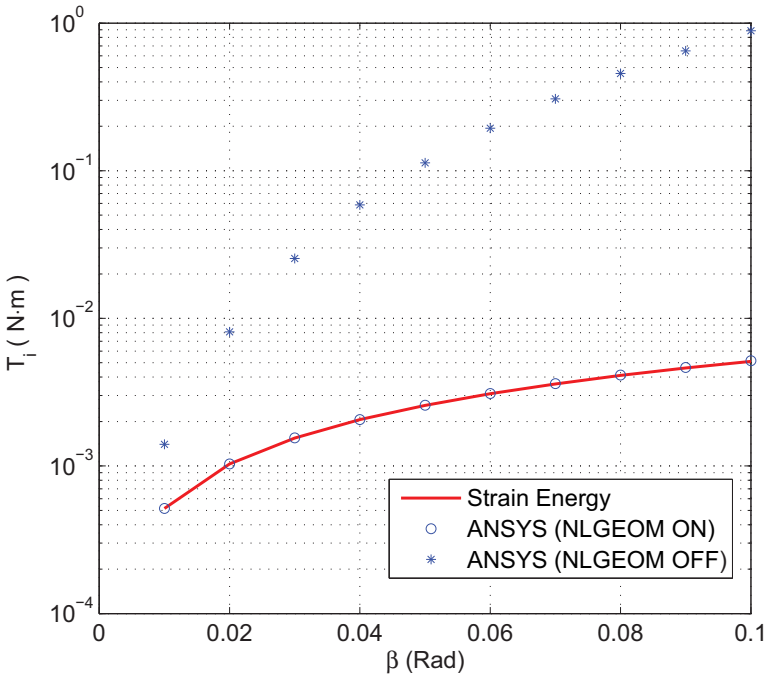

Fig. 5. The input torque versus β.

Table 2 lists the parameters for a circular-guided compliant mechanism. The input torque calculated from Eq. (20) is plotted in Figure 5 as β is increased from 0 to 0.1 Rad (within the BCM's prediction range). The finite element results are also plotted in Figure 5 for the purpose of comparison. The finite element model was built using ANSYS, with the compliant beam being meshed into 150 elements using BEAM188 while the rigid crank modeled by MPC184. The nonlinear finite element results (with NLGEOM, i.e., the geometric nonlinearity option, turned on) verify those obtained by the strain energy method. However, the finite element results with NLGEOM turned off dramatically deviate from the other results, indicating that geometric nonlinearities play an important role in the kinetostatic behaviors of the mechanism.

4.2 Compliant Slant Parallelogram Mechanism

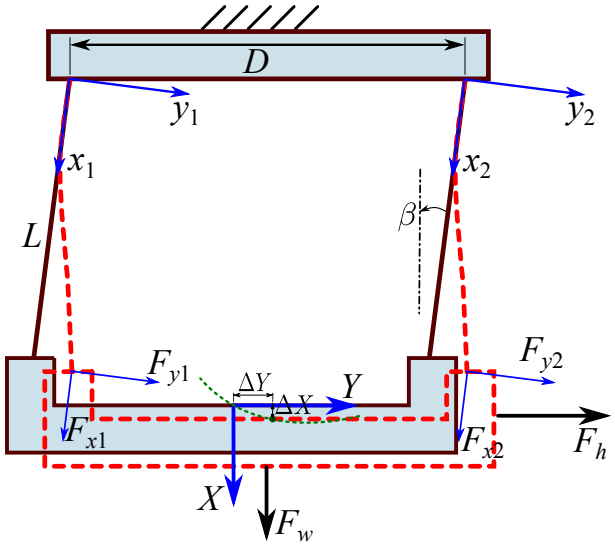

Fig. 6. Compliant slant parallelogram mechanism.

The second example, as illustrated in Figure 6, is a compliant slant parallelogram mechanism often used for accurate positioning. Two compliant beams support a heavy rigid coupler. At the undeflected position, the angles of the two compliant beams with respect to vertical is β. The two beams are identical in cross section (with thickness $T_1 = T_2 = T$ and width $W_1 = W_2 = W$) and length ($L_1 = L_2 = L$). We also have $k_{a1} = k_{a2} = k_a$. The weight of the lower rigid coupler is denoted as F_w. When a horizontal force F_h is applied on the coupler, it will deviate from its undeflected position and the displacement components along the $X-$ and the $Y-$ directions are denoted by Δ_x and Δ_y, respectively.

Considering that the two compliant beams are subject to the same loading condition, we have

$$\begin{aligned} F_{x1} = F_{x2} &= \frac{F_w \cos\beta}{2} - \frac{F_h \sin\beta}{2} \\ F_{y1} = F_{y2} &= \frac{F_w \sin\beta}{2} + \frac{F_h \cos\beta}{2} \end{aligned} \tag{22}$$

In the following, because of symmetry, we only consider the left beam in the modeling.

The complementary strain energy in the left beam is expressed using Eq. (16) (it is more accurate if Eq. (17), i.e., the complementary energy expression with the terms up to the third power in f_x, is used) as

$$\begin{aligned} \bar{v}_1 = &\frac{f_{x1}^2}{2}\left(\frac{1}{k_a} + \frac{17}{315}f_{y1}^2 + \frac{61}{360}f_{y1}m_{z1} + \frac{2}{15}m_{z1}^2\right) - \\ &f_{x1}\left(\frac{1}{15}f_{y1}^2 + \frac{5}{24}f_{y1}m_{z1} + \frac{1}{6}m_{z1}^2\right) + \left(\frac{1}{6}f_{y1}^2 + \frac{1}{2}f_{y1}m_{z1} + \frac{1}{2}m_{z1}^2\right) \end{aligned} \tag{23}$$

Due to $\theta_{z1} = 0$, according to the Crotti-Engesser theorem, we have

$$\begin{aligned} \theta_{z1} &= \frac{d\bar{v}_1}{dm_{z1}} \\ &= \left(1 - \frac{f_{x1}}{3} + \frac{2f_{x1}^2}{15}\right)m_{z1} + \left(\frac{1}{2} - \frac{5f_{x1}}{24} + \frac{61f_{x1}^2}{720}\right)f_{y1} = 0 \end{aligned} \tag{24}$$

Table 3. Parameters of the compliant slant parallelogram mechanism

E	L	W	T	β	F_w
73 GPa	25 mm	5.1 mm	0.25 mm	0.1	0.25 N

Solving Eq. (24) for m_{z1} yields

$$m_{z1} = \frac{61f_{x1}^2 - 150f_{x1} + 360}{-96f_{x1}^2 + 240f_{x1} - 720} f_{y1} \tag{25}$$

Using the Crotti-Engesser theorem,

$$\begin{aligned} u_{x1} = \frac{d\bar{v}_1}{df_{x1}} = &\left(\frac{1}{k_a} + \frac{17f_{y1}^2}{315} + \frac{61f_{y1}m_{z1}}{360} + \frac{2m_{z1}^2}{15} \right) f_{x1} - \\ &\left(\frac{f_{y1}^2}{15} + \frac{5f_{y1}m_{z1}}{24} + \frac{m_{z1}^2}{6} \right) \end{aligned} \tag{26}$$

and

$$\begin{aligned} u_{y1} &= \frac{d\bar{v}_1}{df_{y1}} \\ &= \left(\frac{61f_{x1}^2}{720} - \frac{5f_{x1}}{24} + \frac{1}{2} \right) m_{z1} + \left(\frac{17f_{x1}^2}{315} - \frac{2f_{x1}}{15} + \frac{1}{3} \right) f_{y1} \end{aligned} \tag{27}$$

By substituting Eqs. (22) and (25) into Eqs. (26) and (27), the path of the rigid part can be expressed as a function of F_h (for known constant F_w):

$$\Delta Y = L(-u_{x1}\sin\beta + u_{y1}\cos\beta) \tag{28}$$

and

$$\Delta X = L(u_{x1}\cos\beta + u_{y1}\sin\beta) \tag{29}$$

Table 3 gives the parameters of a compliant slant parallelogram mechanism. For F_h increased from 0 to 1 N in 10 equal steps, Figure 7 plots the coupler's loci of the mechanism obtained by the Crotti-Engesser theorem combined with the complementary energy expressions with terms up to the second and the third powers in f_x, respectively. The finite element model for the compliant slant parallelogram mechanism was built using ANSYS, with each compliant beam being meshed into 150 elements using BEAM188. The nonlinear finite element results (with NLGEOM turned on) verify those of the complementary strain energy method, and show that the complementary energy expression with terms up to the third power in f_x is more accurate than the expression with terms up to the second power.

To further demonstrate the dual relation of the two theorems, the mechanism is analyzed using the strain energy expression using Castigliano's theorem and the results are compared to those obtained by the complementary energy expression

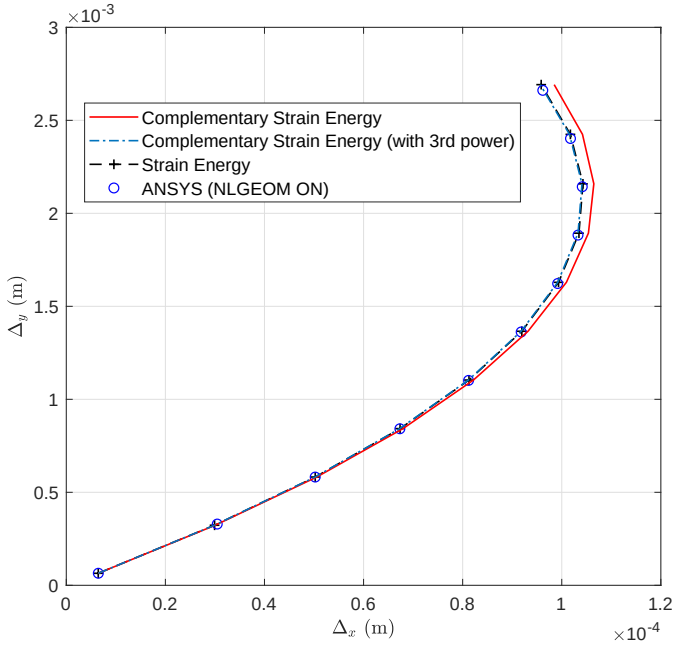

Fig. 7. The coupler's locus of the compliant slant parallelogram mechanism.

and the Crotti-Engesser theorem. Considering the tip angle θ_z of the beam is 0, the normalized strain energy can be expressed as

$$v_1 = \frac{k_a(2u_{x1} + S^{(1)})^2}{8(1 - k_a S^{(2)})} + \frac{S^{(0)}}{2} \tag{30}$$

in which

$$S^{(0)} = 12u_{y1}^2, \;\; S^{(1)} = \frac{6}{5}u_{y1}^2, \;\; S^{(2)} = -\frac{1}{700}u_{y1}^2 \tag{31}$$

Using Castigliano's first theorem on Eq. (30) yields the expressions for the normalized loads exerted on the left beam:

$$\begin{aligned} f_{x1} &= \frac{\partial v_1}{\partial u_{x1}} = \frac{k_a(700u_{x1} + 420u_{y1}^2)}{700 + u_{y1}^2} \\ f_{y1} &= \frac{\partial v_1}{\partial u_{y1}} = \frac{k_a(840u_{x1} + 504u_{y1}^2)}{700 + u_{y1}^2} - \frac{7k_a u_{y1}(10u_{x1} + 6u_{y1}^2)^2}{(700 + u_{y1}^2)^2} + 12u_{y1} \end{aligned} \tag{32}$$

The two equations in Eq. (32) have to be solved simultaneously to obtain the deflections of the beam (u_{x1} and u_{y1}) for given F_h. Then the locus of the coupler is achieved using Eq. (28) and Eq. (29), which is overlaid on the results in Figure 7. The locus agrees well with those obtained by the complementary energy expression with terms up to the third power in f_x and the nonlinear finite element model.

5 Conclusions

An energy-based kinetostatic modeling framework for compliant mechanisms was created by combining concepts from Castigliano's first theorem, the Crotti-Engesser theorem, the beam constraint model, strain energy and complementary strain energy. The strain energy in terms of deflections and the complementary strain energy in terms of loads were derived based on the beam constraint model to facilitate the use of the two theorems in the framework. The kinetostatic modeling of two compliant mechanisms demonstrated the effectiveness of the framework to create explicit formulations and the results were verified through comparison to nonlinear finite element analysis.

It should be noted that the framework is only applied to problems in which the loads are applied at the tips of the flexible beams and the deflections are restricted to their intermediate range because the strain energy and the complementary strain energy are formulated based on the BCM. Nevertheless, it can be extended for large deflections by following the idea of CBCM [3, 24]. The expressions can also facilitate the use of the principle of minimum energy and the principle of minimum complementary energy in the framework, thus setting a foundation for future work. This will also enable incorporation of newly developed optimization techniques for solving kinetostatic problems of compliant mechanisms.

Acknowledgements

The authors gratefully acknowledge the financial support from the National Key R&D Program of China under Grant No. 2019YFB1311600, the National Natural Science Foundation of China under Grant Nos. U1913213 and 51675396, and the grant for Distinguished Young Scholars of Shaanxi Province under Grand No. 2019JC-04.

References

[1] Howell, L. L., 2001. *Compliant Mechanisms*. Wiley, New York.

[2] Turkkan, O. A., and Su, H.-J., 2016. "Das-2d: a concept design tool for compliant mechanisms". *Mechanical Sciences,* **7**(2), pp. 135–148.

[3] Ma, F., and Chen, G., 2016. "Modeling large planar deflections of flexible beams in compliant mechanisms using chained beam-constraint-model". *ASME J. Mech. Robot.,* **8**(2), p. 021018.

[4] Chen, G., and Ma, F., 2015. "Kinetostatic modeling of fully compliant bistable mechanisms using timoshenko beam constraint model". *ASME J. Mech. Des.,* **137**(2), p. 022301.

[5] Dunning, A. G., Tolou, N., Pluimers, P. P., Kluit, L. F., and Herder, J. L., 2012. "Bistable compliant mechanisms: Corrected finite element modeling for stiffness tuning and preloading incorporation". *ASME J. Mech. Des.,* **134**(8), p. 084502.

[6] Zhang, H., Zhu, B., and Zhang, X., 2019. "Origami kaleidocycle-inspired symmetric multistable compliant mechanisms". *ASME J. Mech. Robot.,* **11**(1), p. 011009.

[7] Li, Z., and Bai, S., 2020. "Nonlinear stiffness analysis of spring-loaded inverted slider crank mechanisms with a unified model". *ASME J. Mech. Robot.,* **12**(online), p. 10.1115/1.4045649.

[8] Li, Q., Xu, L., Chen, Q., and Chai, X., 2019. "Analytical elastostatic stiffness modeling of overconstrained parallel manipulators using geometric algebra and strain energy". *ASME J. Mech. Robot.,* **11**(5), p. 051014.

[9] Awtar, S., and Sen, S., 2010. "A generalized constraint model for two-dimensional beam flexures: Nonlinear strain energy formulation". *Journal of mechanical Design,* **132**(8), p. 081009.

[10] Nishiwaki, S., Frecker, M. I., Min, S., and Kikuchi, N., 1998. "Topology optimization of compliant mechanisms using the homogenization method". *International Journal for Numerical Methods in Engineering,* **42**(3), pp. 535–559.

[11] Li, Q., Pan, C., and Xu, X., 2013. "Closed-form compliance equations for power-function-shaped flexure hinge based on unit-load method". *Precision Engineering,* **37**(1), pp. 135–145.

[12] Saxena, A., and Ananthasuresh, G. K., 2000. "On an optimal property of compliant topologies". *Structural and Multidisciplinary Optimization,* **19**(1), pp. 36–49.

[13] Lobontiu, N., Paine, J. S. N., Garcia, E., and Goldfarb, M., 2001. "Corner-filleted flexure hinges". *ASME J. Mech. Des.,* **123**(9), pp. 346–352.

[14] Eastwood, K. W., Francis, P., Azimian, H., Swarup, A., Looi, T., Drake, J. M., and Naguib, H. E., 2018. "Design of a contact-aided compliant notched-tube joint for surgical manipulation in confined workspaces". *ASME J. Mech. Robot.,* **10**(1), p. 015001.

[15] Timoshenko, S., 1940. *Strength of materials Part 1*. D. Van Nostrand Company, New York.

[16] Timoshenko, S. P., and Young, D. H., 1945. *Theory of structures*. McGraw-Hill.

[17] Jennings, A., 1967. "Energy theorems in structural mechanics". *Journal of Engineering Mathematics,* **1**(4), pp. 307–326.

[18] Jensen, B. D., and Howell, L. L., 2003. "Identification of compliant pseudo-rigid-body mechanism configurations resulting in bistable behavior". *ASME J. Mech. Des.,* **125**(3), pp. 701–708.

[19] Aten, Q. T., Zirbel, S. A., Jensen, B. D., and Howell, L. L., 2011. "A numerical method for position analysis of compliant mechanisms with more degrees of freedom than inputs". *ASME Journal of Mechanical Design,* **133**(6), p. 061009.

[20] Venkiteswaran, V. K., Turkkan, O. A., and Su, H.-J., 2017. "Speeding up topology optimization of compliant mechanisms with a pseudorigid-body model". *ASME J. Mech. Robot.,* **9**(4), p. 041007.

[21] Zhang, A., and Chen, G., 2013. "A comprehensive elliptic integral solution to the large deflection problems of thin beams in compliant mechanisms". *ASME J. Mech. Robot.,* **5**(2), p. 021006.

[22] Chen, G., and Zhang, A., 2011. "Accuracy evaluation of prbm for predicting kinetostatic behavior of flexible segments in compliant mechanisms". In Proceedings of the ASME 2011 International Design Engineering Technical Conferences and Computers and Information in Engineering Conference, August 28-31, Washington, DC, USA, pp. DETC2011–47117.

[23] Awtar, S., Slocum, A. H., and Sevincer, E., 2007. "Characteristics of beam-based flexure modules". *ASME J. Mech. Des.,* **129**(6), pp. 625–639.

[24] Chen, G., Ma, F., Hao, G., and Zhu, W., 2019. "Modeling large deflections of initially curved beams in compliant mechanisms using chained beam-constraint-model". *ASME J. Mech. Rob.,* **11**(1), p. 011002.

[25] Bai, R., Awtar, S., and Chen, G., 2019. "A closed-form model for nonlinear spatial deflections of rectangular beams in intermediate range". *International Journal of Mechanical Sciences,* **160**, pp. 307–315.

[26] Chen, G., and Bai, R., 2016. "Modeling large spatial deflections of slender bisymmetric beams in compliant mechanisms using chained spatial-beam-constraint-model". *ASME J. Mech. Robot.,* **8**(4), p. 041011.

[27] Liu, L., Bi, S., Yang, Q., and Wang, Y., 2014. "Design and experiment of generalized triple-cross-spring flexure pivots applied to the ultra-precision instruments". *Review of Scientific Instruments,* **85**(10), p. 105102.

List of Figures

List of Tables